ATBD for Prototype GSICS SEVIRI-IASI Inter-Calibration

Document Change Record

Issue / Revision	*Date*	*DCN. No*	*Summary of Changes*
v1	2010-12-13		Original based on generic template from report titled "Generic ATBD for EUMETSAT's Inter-Calibration of SEVIRI-IASI" EUM/MET/REP/08/0468, v4b, 2010-05-28. Clarified parts related to producing GSICS Correction coefficients and Bias Monitoring.
v2	2010-12-15		Only algorithm implementation v0.3 selected

Table of Contents

0   INTRODUCTION

The Global Space-based Inter-Calibration System (GSICS) aims to inter-calibrate a diverse range of satellite instruments to produce corrections ensuring their data are consistent, allowing them to be used to produce globally homogeneous products for environmental monitoring. Although these instruments operate on different technologies for different applications, their inter-calibration can be based on common principles: Observations are collocated, transformed, compared and analysed to produce calibration correction functions, transforming the observations to common references. To ensure the maximum consistency and traceability, it is desirable to base all the inter-calibration algorithms on common principles, following a hierarchical approach, described here.

This algorithm is defined as a series of generic *steps*:
1) Subsetting
2) Collocating
3) Transforming
4) Filtering
5) Monitoring
6) Correcting

Each step comprises a number of discrete components, outlined in the contents.

Each component can be defined in a hierarchical way, starting from purposes, which apply to all inter-calibrations, building up to implementation details for specific instrument pairs:
i.   Describe the purpose of each component in this generic data flow.
ii.   Provide different options for how these may be implemented in general.
iii. Recommend procedures for the inter-calibration class (e.g. GEO-LEO).
iv.   Provide specific details for each instrument pair (e.g. SEVIRI-IASI).

The implementation of the algorithm need only follow the overall logic – so the components need not be executed strictly sequentially. For example, some parts may be performed iteratively, or multiple components may be combined within a single loop in the code.

0.1   EUMETSAT's Meteosat SEVIRI-IASI Inter-Calibration Algorithm

This document forms the Algorithm Theoretical Basis Document (ATBD) for the inter-calibration of the infrared channels of SEVIRI on the Geostationary (GEO) Meteosat Second Generation satellites with the Infrared Atmospheric Sounding Interferometer (IASI) on board LEO Metop satellites. This document refers only to the prototype implementation, distributed as the GSICS *Demonstration* product, previously described as v0.3 in EUMETSAT [2009].

This is implemented in the IDL suite ICESI (Inter-Calibration EUMETSAT SEVIRI-IASI), which is documented in Annex A. This allows routine, automatic processing of data delivered by standing orders set up on EUMETSAT's Unified Meteorological Archive and Retrieval Facility (U-MARF) after conversion to netCDF formats. Many components of the inter-calibration have been revised when coding this algorithm.
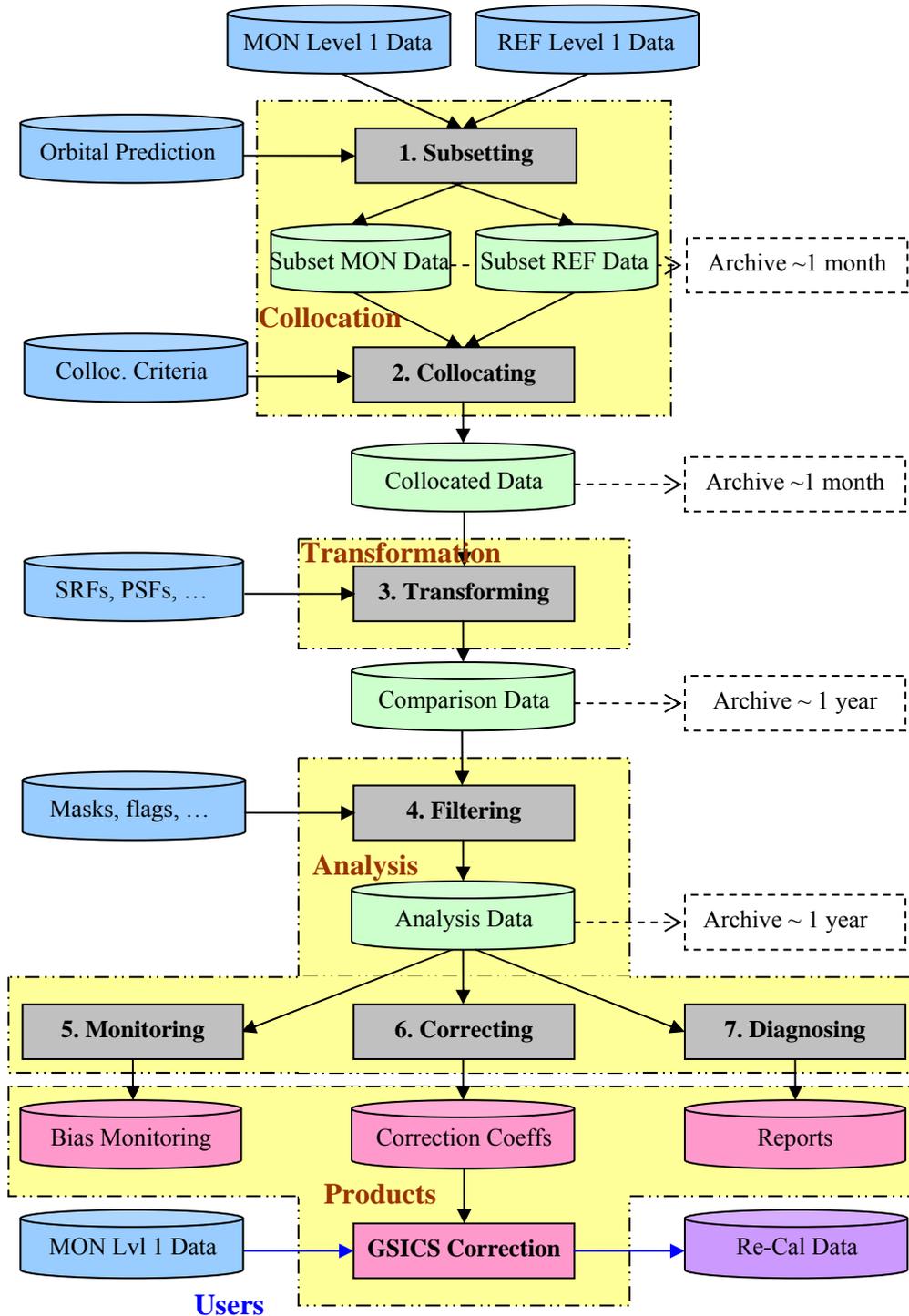
Figure 1: Diagram of generic data flow for inter-calibration of monitored (MON) instrument with respect to reference (REF) instrument

1. SUBSETTING

Acquisition of raw satellite data is obviously a critical first step in an inter-calibration method based on comparing collocated observations. To facilitate the acquisition of data for the purpose of inter-comparison of satellite instruments, prediction of the time and location of collocation events is also important.
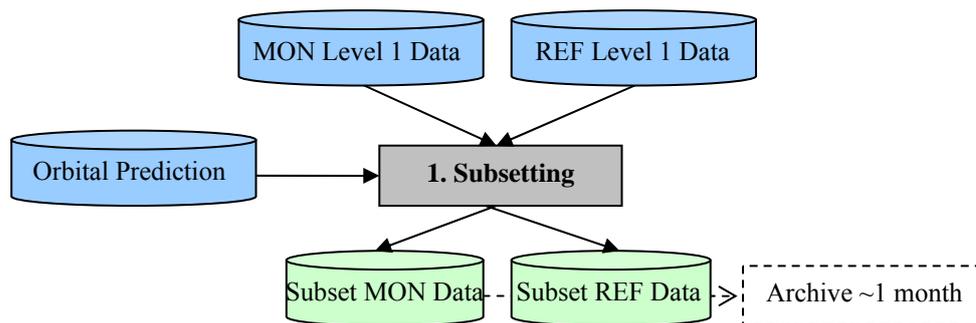
Figure 2: Step 1 of Generic Data Flow, showing inputs and outputs.
MON refers to the monitored instrument. REF refers to the reference instrument.

1.a.   Select Orbit

1.a.i. Purpose

We first perform a rough cut to reduce the data volume and only include relevant portions of the dataset (channels, area, time, viewing geometry). The purpose is to select portions of data collected by the two instruments that are likely to produce collocations. This is desirable because typically less than 0.1% of measurements are collocated. The processing time is reduced substantially by excluding measurements unlikely to produce collocations.

Data is selected on a per-orbit or per-image basis. To do this, we need to know how often to do inter-calibration – which is based on the observed rate of change and must be defined iteratively with the results of the inter-calibration process (see 1.a).

1.a.ii. General Options

The simplest, but inefficient approach is "trial-and-error", i.e., compare the time and location of all pairs of files within a given time window.

1.a.iii. Infrared GEO-LEO inter-satellite/inter-sensor Class

For inter-calibrations between geostationary and sun-synchronous satellites, the orbits provide collocations near the GEO Sub-Satellite Point (SSP) within fixed time windows every day and night. In this case, we adopt the simple approach outlined above.

We define the GEO Field of Regard (FoR) as an area close to the GEO Sub-Satellite Point (SSP), which is viewed by the GEO sensor with a zenith angle less than a threshold. Wu [2009] defined a threshold angular distance from nadir of less than 60° based on geometric considerations, which is the maximum incidence angle of most LEO sounders. This corresponds to $\approx \pm 52°$ in latitude and longitude from the GEO SSP. The GEO and LEO data is then subset to only include observations within this FoR within each inter-calibration period.

Mathematically, the GEO FoR is the collection of locations whose arc angle (angular distance) to nadir is less than a threshold or, equivalently, the cosine of this angle is larger than **min_cos_arc**. We chose the threshold **min_cos_arc = 0.5**, i.e., angular distance less than **60 degree**.

Computationally, with known Earth coordinates of GEO nadir *G* (0, geo_nad_lon) and granule centre *P* (gra_ctr_lat, gra_ctr_lon) and approximating the Earth as being spherical, the arc angle between a LEO pixel and LEO nadir can be computed with cosine theorem for a right angle on a sphere (see Figure 2):

$$\textbf{\textit{Equation 1 }} \cos(GP) = \cos(gra\_ctr\_lat)\cos(geo\_nad\_lon - gra\_ctr\_lon)$$

If the LEO pixel is outside of GEO FoR, no collocation is considered possible. Note the arc angle *GP* on the left panel of Figure 2, which is the same as the angle $\angle GOP$ on the right panel, is smaller than the angle $\angle SPZ$ (right panel), the zenith angle of GEO from the pixel. This means that the instrument zenith angle is always less than 60 degrees for all collocations.
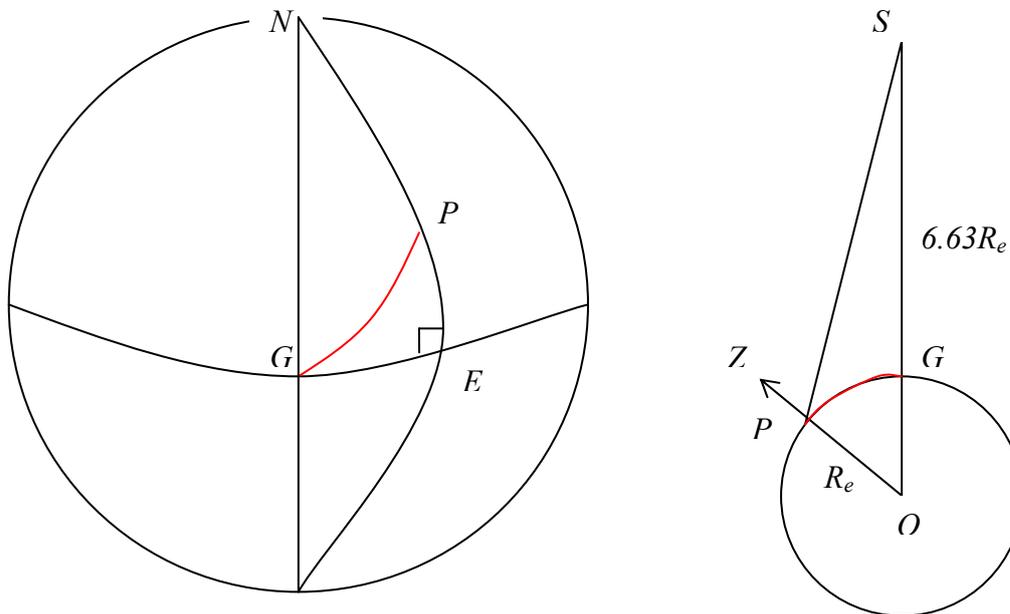
Figure 3: Computing arc angle to satellite nadir and zenith angle of satellite from Earth location

1.a.iv. Specifics for Prototype SEVIRI-IASI

For SEVIRI, the GEO FoR is further reduced to include only data within ±30° lat/lon of the SSP. A single Metop overpass is selected with a night-time equator crossing closest to the GEO SSP. The IASI data within this overpass is then geographically subset to only include data within this smaller GEO FoR by applying time filtering. This is implemented as a standing order from EUMETSAT's Unified Meteorological Archive and Retrieval Facility (U-MARF) delivering data in NetCDF format every night, as described in Annex A.

The subset of 7 Meteosat images shall be extracted with equator crossing times closest to the mean observation time within each subset IASI orbit.

2. FIND COLLOCATIONS

A set of observations from a pair of instruments within a common period (e.g. 1 day) is required as input to the algorithm. The first step is to obtain these data from both instruments, select the relevant comparable portions and identify the pixels that are spatially collocated, temporally concurrent, geometrically aligned and spectrally compatible and calculate the mean and variance of these radiances.
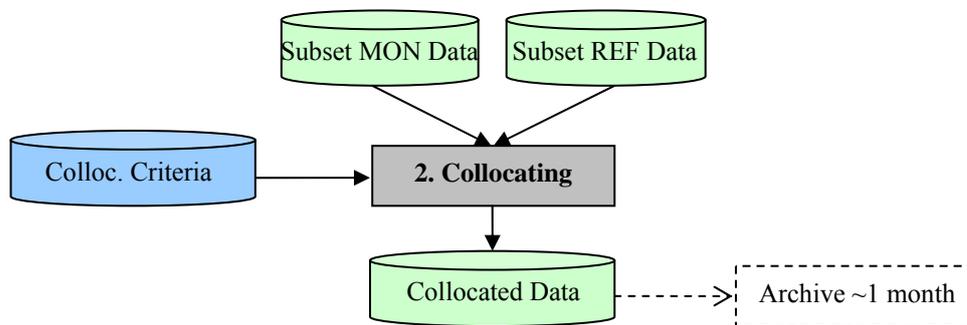
Figure 4: Step 2 of Generic Data Flow, showing inputs and outputs

2.a.   Collocation in Space

2.a.i.   Purpose

The following components of this step define which pixels can be used in the direct comparison. To do this, we first extract the central location of each instruments' pixels and determine which pixels can considered to be collocated, based on their centres being separated by less than a pre-determined threshold distance. At the same time we identify the pixels that define the target area (FoV) and *environment* around each collocation. These are later averaged in 3.c.

The *target area* is defined to be a little larger than the larger Field of View (FoV) of the instruments so it covers all the contributing radiation in event of small navigation errors, while being large enough to ensure reliable statistics of the variance are available. The exact ratio of the target area to the FoV will be instrument-specific, but in general will range 1 to 3 times the FoV, with a minimum of 9 'independent' pixels.

2.a.ii. General Options

An efficient method of searching for collocations is to calculate 2D-histograms of the locations of both instruments' observations on a common grid in latitude/longitude space. Non-zero elements of both histograms identify the location of collocated pixels and their indices provide the coordinates in observation space (scan line, element, FoV, …). However, this does not capture pixel pairs that straddle bin boundaries of the histograms.

2.a.iii. Infrared GEO-LEO inter-satellite/inter-sensor Class

The spatial collocation criteria is based on the nominal radius of the LEO FoV at nadir. This is taken as a threshold for the maximum distance between the centre of the LEO and GEO pixels for them to be considered spatially collocated. However, given the geometry of the already subset data, it is assumed that all LEO pixels within the GEO FoR will be within the threshold distance from a GEO pixel. The GEO pixel closest to the centre of each LEO FoV can be identified using a reverse look-up-table (e.g. using a McIDAS function).

2.a.iv. Specifics for Prototype SEVIRI-IASI

The IASI iFoV is defined as a circle of 12 km diameter at nadir. The SEVIRI FoV is defined as square pixels with dimensions of 3x3 km at SSP. An array of 5x5 SEVIRI pixels centred on the pixel closest to centre of each IASI pixel are taken to represent both the IASI iFoV and its *environment*.

SEVIRI and IASI pixels are selected that fall within the same bin of a 2-D histograms with 0.125° lat/lon grid, covering ±35° lat/lon. This is implemented in the routine **icesi_collocate** (see Annex A).

2.b.   Concurrent in Time

2.b.i. Purpose

Next we need to identify which of those pixels identified in the previous step as spatially collocated are also collocated in time. Although even collocated measurements at very different times may contribute to the inter-calibration, if treated properly, the capability of processing collocated measurements is limited and the more closely concurrent ones are more valuable for the inter-calibration.

2.b.ii. General Options

Each pixel identified as being spatially collocated is tested sequentially to check whether the observations from both instruments were sampled sufficiently closely in time – i.e. separated in time by no more than a specific threshold. This threshold should be chosen to allow a sufficient number of collocations, while not introducing excessive noise due to temporal variability of the target radiance relative to its spatial variability on a scale of the collocation target area – see Hewison [2009a].

2.b.iii. Infrared GEO-LEO inter-satellite/inter-sensor Class

The time at which each collocated pixel of the GEO image was sampled is extracted or calculated and compared to for the collocated LEO pixel. If the difference is greater than a threshold of 300s, the collocation is rejected, otherwise it is retained for further processing.

Equation 2: $\left| LEO\_time - GEO\_time \right| < \max\_\sec$, where *max_sec*=300s

The problem with applying a time collocation criteria in the above form is that it will often lead to only a part of the collocated pixels being analysed. As the GEO image is often climatologically asymmetric about the equator, this can lead to the collocated radiances having different distributions, which can affect the results. A possible solution to this problem is to apply the time collocation to the average sample time of both the GEO and LEO data. This would ensure either all or none of the pixels within each overpass are considered to be collocated in time. However, this is not implemented in this version.

2.b.iv. Specifics for Prototype SEVIRI-IASI

The time at which each collocated pixel of the SEVIRI image was sampled is approximated by interpolating between the sensing start and end time given in the meta data, according to the scan line number, which increments linearly from 1, just 'below' the South Pole to 3712, just 'above' the North Pole in a period of 742.4 s for a full disk scan. This is compared to the sample time given in the IASI Level 1.5c dataset. If the difference is greater than a threshold of *max_sec*=900s, the collocation is rejected, otherwise it is retained for further processing. This is implemented in the routine **icesi_collocate** (see Annex A).

2.c.   Alignment in Viewing Geometry

2.c.i.   Purpose

The next step is to ensure the selected collocated pixels have been observed under comparable conditions. This means they should be aligned such that they view the surface at similar incidence angles (which may include azimuth and polarisation as well as elevation angles) through similar atmospheric paths.

2.c.ii.   General Options

Each pixel identified as being spatially and temporally collocated is tested sequentially to check whether the viewing geometry of the observations from both instruments was sufficiently close. The criterion for zenith angle is defined in terms of atmospheric path length, according to the difference in the secant of the observations' zenith angles and the difference in azimuth angles. If these are less than pre-determined thresholds the collocated pixels can be considered to be aligned in viewing geometry and included in further analysis. Otherwise they are rejected.

2.c.iii. Infrared GEO-LEO inter-satellite/inter-sensor Class

The geometric alignment of thermal infrared channels depends only on the zenith angle and not azimuth or polarisation.

Equation 3: $\left| \dfrac{\cos(geo\_zen)}{\cos(leo\_zen)} - 1 \right| < \max\_zen$

The threshold value for *max_zen* can be quite large for window channels (e.g., 0.05 for 10.8 μm channel) but must be rather small for more absorptive channels (e.g., <0.02 for 13.4 μm channel). However, unless there are particular needs to increase the sample size for window channels, a common threshold value of *max_zen*=0.01 is recommended for all channels. This results in collocations being distributed approximately symmetrically about the equator mapping out a characteristic *slanted hourglass* pattern.

Another aspect of viewing geometry alignment is azimuth angle. Similar zenith angle assures similar path length; additional requirement of similar azimuth angle assures similar line-of-sight. Line-of-sight alignment is relevant for IR spectrum in certain cases. For infrared window channels, land surface emission during daytime may be anisotropic [Minnis *et al.* 2004]. For shortwave IR band (e.g., 4 μm), azimuth angle alignment is required during daytime when solar radiation is considerable. It is, therefore recommended that inter-calibration over land and in this band are limited to night-time only cases – at the expense of limiting the dynamic range of the results.

2.c.iv. Specifics for Prototype SEVIRI-IASI

Implemented as above, using *max_zen*=0.01, in the routine **icesi_collocate** (see Annex A).

2.d.   Pre-Select Channels

2.d.i. Purpose

Only broadly comparable channels from both instruments are selected to reduce data volume.

2.d.ii. General Options

This selection is based on pre-determined criteria for each instrument pair.

2.d.iii. Infrared GEO-LEO inter-satellite/inter-sensor Class

Only the channels of the GEO and LEO sensors are selected in the thermal infrared range of 3-15µm.

2.d.iv. Specifics for Prototype SEVIRI-IASI

Select SEVIRI's infrared channels: 3.9, 6.2, 7.3, 8.7, 9.7, 10.8, 12.0, 13.4 µm. Select all channels for IASI. This selection is implemented in the U-MARF standing orders, as shown in Annex A.
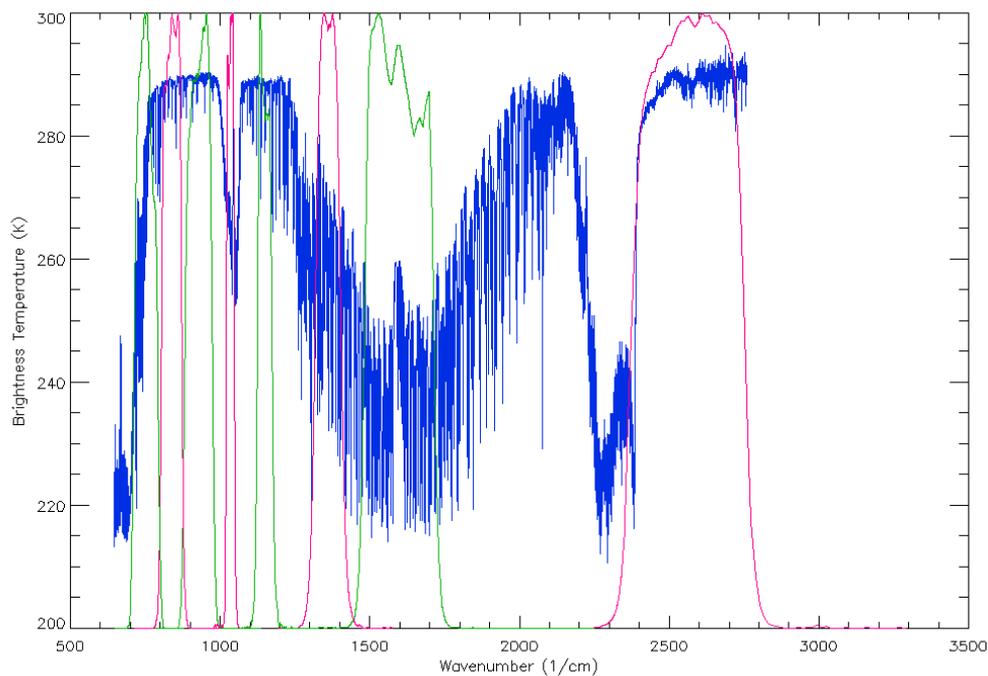

Figure 5: Example radiance spectra measured by IASI (blue), expressed in brightness temperature (K) and Spectral Response Functions of SEVIRI channels 3-11 from right to left (red/green).

2.e.   Plot Collocation Map

2.e.i.   Purpose

When interpreting the inter-calibration results it is often helpful to visualise the distribution of the source data used in the comparison.

2.e.ii. General Options

This can be achieved by producing a map showing the distribution of collocation targets.

2.e.iii. Infrared GEO-LEO inter-satellite/inter-sensor Class

The map is produced showing all the GEO-LEO pixels meeting the collocation criteria every day. These points are overlaid on a background image from an infrared window channel of the GEO instrument. This allows the distribution of cloud to be visualised and considered in the interpretation of the results.

2.e.iv. Specifics for Prototype SEVIRI-IASI

An image is produced of the IR10.8 channel radiance over the GEO FoR on a fixed radiance scale running from 80 mW/m2/st/cm-1 (white) to 140 mW/m2/st/cm-1 (black). The position of the centre of all IASI iFoVs is over-plotted on this image in grey and those pixels meeting the collocation criteria are over-plotted in red, as shown in Figure 6.
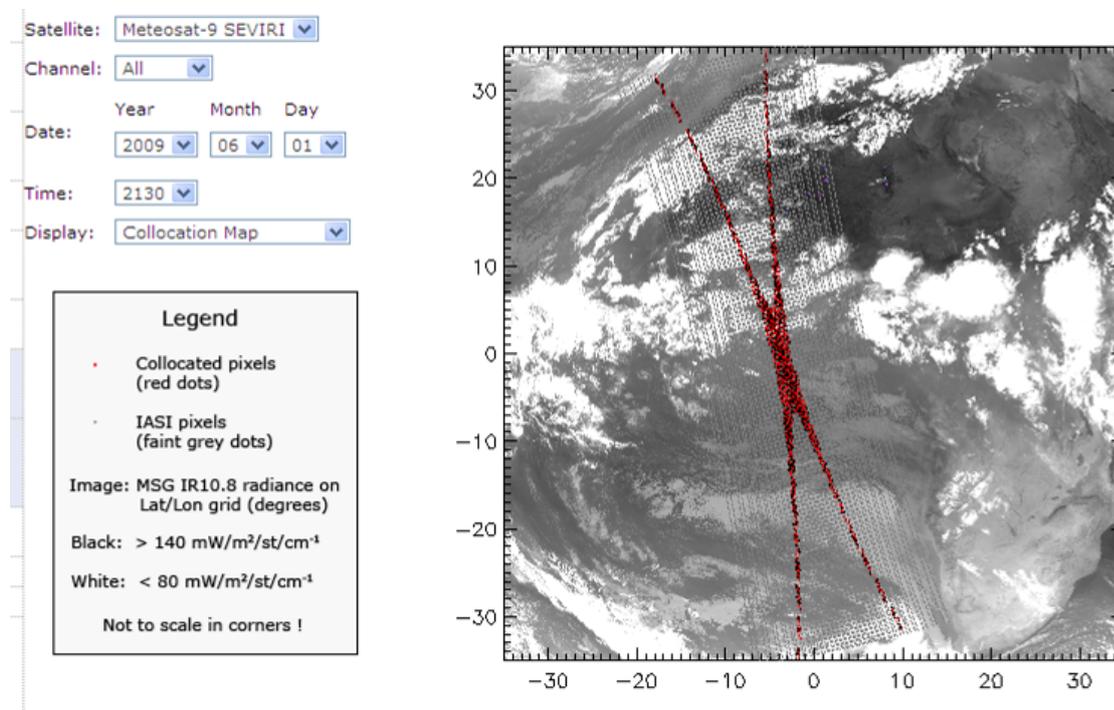
Figure 6: Example collocation map, follow inset legend.

3. TRANSFORM DATA

In this step, collocated data are transformed to allow their direct comparison. This includes modifying the spectral, temporal and spatial characteristics of the observations, which requires knowledge of the instruments' characteristics. The outputs of this step are the best estimates of the channel radiances, together with estimates of their uncertainty.
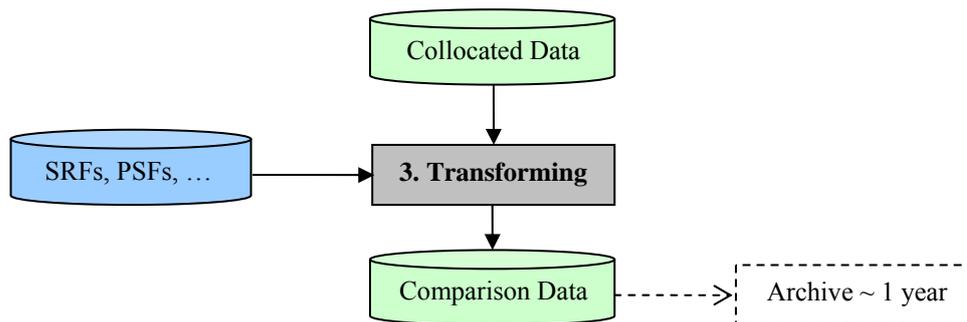
Figure 7: Step 3 of Generic Data Flow, showing inputs and outputs

3.a.   Convert Radiances

3.a.i. Purpose

Convert observations from both instruments to a common definition of radiance to allow direct comparison.

3.a.ii. General Options

The instruments' observations are converted from Level 1.5/1b/1c data to radiances, using pre-defined, published algorithms specific for each instrument.

3.a.iii. Infrared GEO-LEO inter-satellite/inter-sensor Class

Perform comparison in radiance units: $mW/m^2/st/cm^{-1}$.

3.a.iv. Specifics for Prototype SEVIRI-IASI

The Meteosat radiance definition applicable to each level 1.5 dataset, described by EUMETSAT [2010], is used, accounting for the instrument's Spectral Response Functions [EUMETSAT, 2006].

IASI data are converted to radiances using the published algorithm [EUMETSAT, 2008a].

The routines **read_msg_nc** and **read_iasi_nc** read the NetCDF format data.

3.b.   Spectral Matching

3.b.i.   Purpose

Firstly, we must identify which channel sets provide sufficient common information to allow meaningful inter-calibration. These are then transformed into comparable pseudo channels, accounting for the deficiencies in channel matches.

3.b.ii.   General Options

The Spectral Response Functions (SRFs) must be defined for all channels. The observations of channels identified as comparable are then co-averaged using pre-determined weightings to give *pseudo channel* radiances. A Radiative Transfer Model can be used to account for any differences in the pseudo channels' characteristics. The uncertainty due to spectral mismatches is then estimated for each channel.

3.b.iii. Infrared GEO-LEO inter-satellite/inter-sensor Class

For hyper-spectral instruments, all SRFs are first transformed to a common spectral grid. The LEO hyperspectral channels are then convolved with the GEO channels' SRFs to create synthetic radiances in pseudo-channels, accounting for the spectral sampling and stability in an error budget.

Equation 4: $R_{GEO} = \dfrac{\int_{\nu} R_{\nu} \Phi_{\nu} d\nu}{\int_{\nu} \Phi_{\nu} d\nu}$

where R_{GEO} is the simulated GEO radiance, R_{ν} is LEO radiance at wave number ν, and Φ_{ν} is GEO spectral response at wave number ν.

In general LEO hyperspectral sounders do not provide complete spectral coverage of the GEO channels either by design (e.g. gaps between detector bands), or by subsequent hardware failure (e.g. broken or noisy channels). The radiances in these *gap channels* shall be accounted by one of the following techniques:

The simplest option is simply to ignore the contribution from the *gap channels*. This will obviously introduce a bias in the resulting radiances, depending on the specific channels under consideration.

3.b.iv. Specifics for Prototype SEVIRI-IASI

Analysis [Hewison, 2008b] has shown that the contribution of the IR3.9 channel radiance not covered by IASI is small enough (~0.17 K) to be ignored in the prototype code, which is implemented in the **icesi_convolve** routine (see Annex A).

3.c.   Spatial Matching

3.c.i. Purpose

The observations from each instrument are transformed to comparable spatial scales. This involves averaging all the pixels identified in 2 as being within the *target* and *environment* areas. The uncertainty due to spatial variability is estimated.

3.c.ii. General Options

The Point Spread Functions (PSFs) of each instrument are identified. The *target area* and *environment* around it were specified in 2. Now the pixels within these areas are identified and their radiances are averaged and their variance calculated to estimate the uncertainty on the average due to spatial variability, accounting for any over-sampling.

3.c.iii. Infrared GEO-LEO inter-satellite/inter-sensor Class

The *target area* is defined as the nominal LEO FoV at nadir. The GEO pixels within target area are averaged using a uniform weighting and their variance calculated. The *environment* is defined by the GEO pixels within 3x radius of the target area from the centre of each LEO FoV.

3.c.iv. Specifics for Prototype SEVIRI-IASI

The IASI iFoV is defined as a circle of 12km diameter at nadir. The SEVIRI FoV is defined nominally as square pixels with lengths of 3km at SSP. These are assumed to be constant across collocation domain. The *target area* is defined by arrays of 5x5 SEVIRI pixels closest to centre of each IASI iFoV, as shown in Figure 9. This is somewhat larger than the size of the IASI iFoV at nadir, but smaller at the extremes of its scan. The *environment* is not defined, as it is not used in further analysis.

SEVIRI and IASI pixels are selected that fall within the same bin of a 2-D histograms with 0.125° lat/lon grid, covering ±35° lat/lon. This is implemented in the routine **icesi_collocate** (see Annex A) simultaneously with the collocation component (1b).
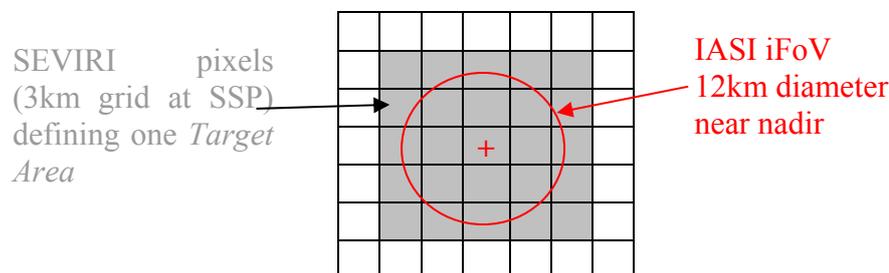

Figure 8: Definition of **Target Area** *as 5x5 SEVIRI pixels to spatially match an IASI iFoV.*

3.d.   Viewing Geometry Matching

3.d.i. Purpose

Despite the collocation criteria described in 2.c, each instrument can measure radiance from the collocation targets in slightly different viewing geometry. It may be possible to account for small differences by considering simplified a radiative transfer model.

3.d.ii. General Options

Differences in viewing geometry within the collocation criteria described in 2.c are assumed to be negligible and ignored in further analysis. Although it may be possible to account for small differences by considering simplified a radiative transfer model this has not been implemented at this time.

3.d.iii. Infrared GEO-LEO inter-satellite/inter-sensor Class

Differences in viewing geometry within the collocation criteria described in 2.c are assumed to be negligible and ignored in further analysis.

3.d.iv. Specifics for Prototype SEVIRI-IASI

As above.

3.e. Temporal Matching

3.e.i. Purpose

Different instruments measure radiance from the collocation targets at different times. The impact of this difference can usually be reduced by careful selection, but not completely eliminated. The timing difference between instruments' observations is established and the uncertainty of the comparison is estimated based on (expected or observed) variability over this timescale.

3.e.ii. General Options

Each instrument's sample timings are identified.

3.e.iii. Infrared GEO-LEO inter-satellite/inter-sensor Class

Only the GEO image closest to the LEO equator crossing time is selected. The time difference between the collocated GEO and LEO observations is neglected and the collocation targets are assumed to be sampled simultaneous, contributing no additional uncertainty to the comparison.

3.e.iv. Specifics for Prototype SEVIRI-IASI

As above.

4. **FILTERING**

The collocated and transformed data will be archived for analysis. Before that, the GSICS inter-calibration algorithm reserves the opportunity to remove certain data that should not be analyzed (quality control), and to add auxiliary data that will add further analysis. For example, it may be useful to incorporate land/sea/ice masks and/or cloud flags to better classify the results.
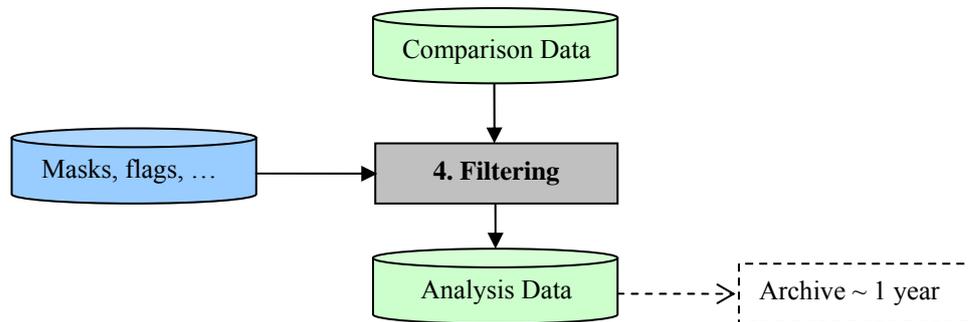

Figure 9: Step 4 of Generic Data Flow, showing inputs and outputs.

4.a.   Uniformity Test

4.a.i.   Purpose

Knowledge of scene uniformity is critical in reducing and evaluating inter-calibration uncertainty. To reduce uncertainty in the comparison due to spatial/temporal mismatches, the collocation dataset may be filtered so only observations in homogenous scenes are compared.

4.a.ii.   General Options

The approach adopted in this version is not to reject collocations based on a threshold of scene variability, but to use scene variances as weightings in the regression of collocated radiances. Comparatively, the threshold option has the theoretical disadvantage of subjectivity but practical advantage of substantially reducing the amount of data to be archived. Recent analysis [Tobin, personal communication, 2009] also indicates that the threshold option is always suboptimal compared to the weight option.

4.a.iii. Infrared GEO-LEO inter-satellite/inter-sensor Class

The variance of the radiances of all the GEO pixels within each LEO FoV is calculated in 3.c.

4.a.iv. Specifics for Prototype SEVIRI-IASI

An option is included to reject any targets where the standard deviation of the scene radiance is >5% of the standard radiance (see 4b). This is implemented as an option (**filter=2**) in the routine **icesi_analyse** (see Annex A).

4.b.   Outlier Rejection

4.b.i. Purpose

To prevent anomalous observations having undue influence on the results, 'outliers' may be identified and rejected on a statistical basis. Small number of anomalous pixels in the environment, even concentrated, may not fail the uniformity test. However, if they appear only in one sensor's field of view but not the other, it can cause unwanted bias in a single comparison.

4.b.ii. General Options

The simplest implementation is to include the outliers in the further analysis. Since the anomaly has equal chance to appear in either sensor's field of view, comparison of large number of samples remains unbiased but has increased noise. This is the recommended approach.

4.b.iii. Infrared GEO-LEO inter-satellite/inter-sensor Class

All inter-calibration targets are included in further analysis, regardless of whether they are outliers with respect to their environment.

4.b.iv. Specifics for Prototype SEVIRI-IASI

No outlier rejection implemented, as recommended above.

4.c.   Auxiliary Datasets

4.c.i.   Purpose

It may be useful to incorporate land/sea/ice masks and/or cloud flags to allow analysis of statistics in terms of other geophysical variables – e.g. land/sea/ice, cloud cover, etc.

It may also be possible to estimate the spatial variability within the LEO FoV from collocated AVHRR observations from the same LEO satellite.

4.c.ii.   General Options

Not yet implemented.

4.c.iii. Infrared GEO-LEO inter-satellite/inter-sensor Class

Not yet implemented.

4.c.iv. Specifics for Prototype SEVIRI-IASI

Not yet implemented.

5. MONITORING

This step includes the actual comparison of the collocated radiances produced in Steps 1-4, the production of statistics summarising the results to be used in the Correcting step, and reporting any differences in ways meaningful to a range of users.
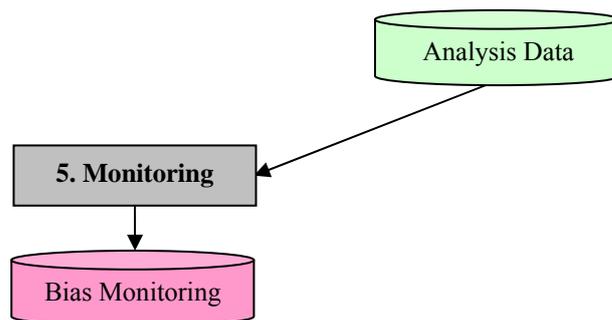
Figure 10: Step 5 of Generic Data Flow, showing inputs and outputs.

5.a. Define Standard Radiances (Offline)

5.a.i. Purpose

This component provides standard reference scene radiances at which instruments' inter-calibration bias can be directly compared and conveniently expressed in units understandable by the users. Because biases can be scene-dependent, it is necessary to define channel-specific *standard radiances*. More than one standard radiance may be needed for different applications – e.g. clear/cloudy, day/night. This component is carried out offline.

5.a.ii. General Options

A representative Region of Interest (RoI) is selected and histograms of the observed radiances within RoI are calculated for each channel. Histogram peaks are identified corresponding to clear/cloudy scenes to define standard radiances. These are determined *a priori* from representative sets of observations.

5.a.iii. Infrared GEO-LEO inter-satellite/inter-sensor Class

As above, but the FoR is limited to within 30° latitude/longitude of the GEO sub-satellite point and times limited to night-time LEO overpasses.

5.a.iv. Specifics for Prototype SEVIRI-IASI

The modes of the histograms of each channels' brightness temperature for collocated pixels in 5 K wide bins from 200 to 300 K are used, as follows:
(For bimodal distributions, the mean of the modes is used.)

Ch (μm)	3.9	6.2	7.3	8.7	9.7	10.8	12.0	13.4
$T_{b\text{std}}$ (K)	290	240	260	290	270	290	290	270

5.b. Regression of Most Recent Results

5.b.i. Purpose

Regression is used as the basis of the systematic comparison of collocated radiances from two instruments. (This comparison may also be done in counts or brightness temperature.) Regression coefficients shall be made available to users to apply the GSICS Correction to the monitored instrument, re-calibrating its radiances to be consistent with those of the reference instrument. Scatterplots of the regression data should also be produced to allow visualisation of the distribution of radiances.

Regressions also allow us to investigate how biases depend on various geophysical variables and provides statistics of any significant dependences, which can used to refine corrections and allows investigation of the possible causes. Such investigations should be carried out offline and may result in future refinements to the ATBD.

5.b.ii. General Options

The recommended approach is to perform a weighted linear regression of collocated radiances. The inverse of the sum of the spatial and temporal variance of the target radiance and the radiometric noise provide an estimated uncertainty on each dependent point, which is used as a weighting. (Including the radiometric noise ensures that very homogeneous targets scenes where all the pixels give the same radiance do not have undue influence on the weighted regression.)

This method produces estimates of regression coefficients describing the slope and offset of the relationship between the two instruments' radiances – together with their uncertainties, expressed as a covariance. The problem of correlation between the uncertainties on each coefficient may be reduced by performing the regression on a transformed dataset – for example, by subtracting the mean or reference radiance from each set.

The observations of the reference instrument, *x*, and monitored instrument, *y*, are fitted to a straight line model of the form:

Equation 5: $\hat{y}(x) = a + bx$

We assume an uncertainty σ_i associated with each measurement, y_i, is known and that the dependent variable, x_i is also known.

To fit the observed data to the above model, we minimise the chi-square merit function:

Equation 6: $\chi^2(a,b) = \sum_{i=1}^{N} \left(\frac{y_i - a - bx_i}{\sigma_i} \right)^2$

This can be implemented following the method described in Section 15.2 of Numerical Recipes [Press *et al.*, 1996], which is implemented in the *POLY_FIT* function of IDL, yielding the following estimates of the regression coefficients:

Equation 7: $a = \dfrac{\sum\limits_{i=1}^{N}\dfrac{x_i^2}{\sigma_i^2}\sum\limits_{i=1}^{N}\dfrac{y_i}{\sigma_i^2} - \sum\limits_{i=1}^{N}\dfrac{x_i}{\sigma_i^2}\sum\limits_{i=1}^{N}\dfrac{x_i\,y_i}{\sigma_i^2}}{\sum\limits_{i=1}^{N}\dfrac{1}{\sigma_i^2}\sum\limits_{i=1}^{N}\dfrac{x_i^2}{\sigma_i^2} - \left(\sum\limits_{i=1}^{N}\dfrac{x_i}{\sigma_i^2}\right)^2}$,

Equation 8: $b = \dfrac{\sum\limits_{i=1}^{N}\dfrac{1}{\sigma_i^2}\sum\limits_{i=1}^{N}\dfrac{x_i\,y_i}{\sigma_i^2} - \sum\limits_{i=1}^{N}\dfrac{x_i}{\sigma_i^2}\sum\limits_{i=1}^{N}\dfrac{y_i}{\sigma_i^2}}{\sum\limits_{i=1}^{N}\dfrac{1}{\sigma_i^2}\sum\limits_{i=1}^{N}\dfrac{x_i^2}{\sigma_i^2} - \left(\sum\limits_{i=1}^{N}\dfrac{x_i}{\sigma_i^2}\right)^2}$,

their uncertainties:

Equation 9: $\sigma_a^2 = \dfrac{\sum\limits_{i=1}^{N}\dfrac{x_i^2}{\sigma_i^2}}{\sum\limits_{i=1}^{N}\dfrac{1}{\sigma_i^2}\sum\limits_{i=1}^{N}\dfrac{x_i^2}{\sigma_i^2} - \left(\sum\limits_{i=1}^{N}\dfrac{x_i}{\sigma_i^2}\right)^2}$,

Equation 10: $\sigma_b^2 = \dfrac{\sum\limits_{i=1}^{N}\dfrac{1}{\sigma_i^2}}{\sum\limits_{i=1}^{N}\dfrac{1}{\sigma_i^2}\sum\limits_{i=1}^{N}\dfrac{x_i^2}{\sigma_i^2} - \left(\sum\limits_{i=1}^{N}\dfrac{x_i}{\sigma_i^2}\right)^2}$,

and their covariance:

Equation 11: $\mathrm{cov}(a,b) = \dfrac{-\sum\limits_{i=1}^{N}\dfrac{x_i}{\sigma_i^2}}{\sum\limits_{i=1}^{N}\dfrac{1}{\sigma_i^2}\sum\limits_{i=1}^{N}\dfrac{x_i^2}{\sigma_i^2} - \left(\sum\limits_{i=1}^{N}\dfrac{x_i}{\sigma_i^2}\right)^2}$.

5.b.iii. Infrared GEO-LEO inter-satellite/inter-sensor Class

Inter-calibrations are repeated daily using only night-time LEO overpasses. Collocations are weighted by the inverse the sum of the spatial and temporal variance of target radiances and their radiometric noise level in the regression. (The inclusion of the radiometric noise ensures the weights never become infinite due to collocation targets with zero variance.) Scatterplots of the regression data should also be produced to allow visualisation of the distribution of radiances, following the example shown in Figure 12.
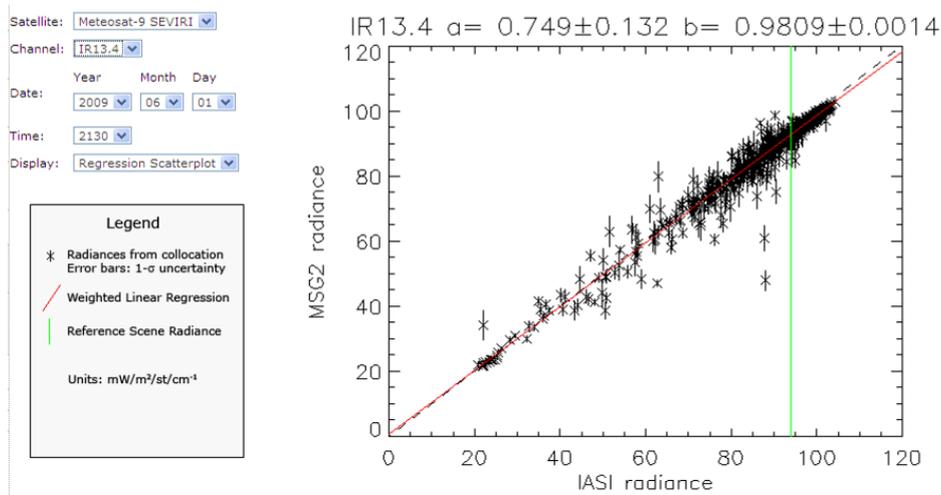
Figure 11: Example scatterplot showing regression of collocated radiances, following legend.

5.b.iv. Specifics for Prototype SEVIRI-IASI

Implemented as above. The range of incidence angles was implicitly extended to <40° by changing the FoR constraints. Inter-calibrations are attempted every day (although only ~½ of cases contain collocations).

This is implemented in the routine **icesi_analyse** (see Annex A).

The temporal variance is assumed to be equal to the spatial variance, so its contribution to the weighting is multiplied by $\sqrt{2}$ and added in quadrature to the radiometric noise. The radiometric noise for IASI is assumed to be negligible when averaged over all channels within the SRF of each SEVIRI channel. The radiometric noise on each pixel for the SEVIRI channels is given by [EUMETSAT, 2007]. For example, for "ambient calibrations" at 95 K:

Channel IR	3.9	6.2	7.3	8.7	9.7	10.8	12.0	13.4
MSG-1 Noise [K]	0.013	0.045	0.065	0.070	0.115	0.065	0.120	0.185
MSG-2 Noise [K]	0.090	0.050	0.050	0.075	0.100	0.070	0.100	0.205

5.c. Bias Calculation

5.c.i. Purpose

Inter-calibration biases should be directly comparable for representative scenes and conveniently expressed in units understandable by the users. Because biases can be scene-dependent, they are evaluated here at the standard radiances defined in 5.a.

5.c.ii. General Options

Regression coefficients are applied to estimate expected bias, $\Delta\hat{y}(x_{STD})$, and uncertainty, $\sigma_{\hat{y}}(x_{STD})$, for standard radiances, accounting for correlation between regression coefficients.

Equation 12: $\Delta\hat{y}(x_{STD}) = a + bx_{STD} - y_{STD}$,

noting that $y_{STD} = x_{STD}$ and

Equation 13: $\sigma_{\hat{y}}^2(x_{STD}) = \sigma_a^2 + \sigma_b^2 x_{STD}^2 + 2\operatorname{cov}(a,b)x_{STD}$

The results may be expressed in absolute or percentage bias in radiance, or brightness temperature differences.

5.c.iii. Infrared GEO-LEO inter-satellite/inter-sensor Class

Biases and their uncertainties are converted from radiances to brightness temperatures for visualisation purposes.

5.c.iv. Specifics for Prototype SEVIRI-IASI

As above, using the definition of effective radiance in the conversion to brightness temperatures [EUMETSAT, 2008b].

5.d.   Consistency Test

5.d.i. Purpose

The most recent results are tested for statistical consistency with the previous time series of results. Users should be alerted to any sudden changes in the calibration of the instruments, allowing them to investigate potential causes and *reset trend* statistics calculated in 5.e. The consistency test may be performed in terms of regression coefficients or biases.

5.d.ii. General Options

The biases calculated for standard radiances from the most recent collocations are compared to the statistics of the biases' trends calculated in 5.e from previous results. If the most recent result falls outside the 3-σ (99.7%) confidence limits estimated from the trend statistics, an alert should be raised. This alert should trigger the Principle Investigator to check the cause of the change and reset the trends by issuing a *trend reset*.

$$\textbf{Equation 14:} \quad \left| \frac{y_i - \hat{y}_i(x_i)}{\sigma_{\hat{y}(x_i)}} \right| \ge Gaussian(=3)$$

5.d.iii. Infrared GEO-LEO inter-satellite/inter-sensor Class

As above.

5.d.iv. Specifics for Prototype SEVIRI-IASI

Implemented as above.

5.e. Trend Calculation

5.e.i. Purpose

It is important to establish whether an instrument's calibration is changing slowly with time. It is possible to establish this from a time-series of inter-comparisons by calculating a trend line using a linear regression with date as the independent variable. Only the portion of the time series since the most recent *trend reset* is analysed, to allow for step changes in the instruments' calibration.

5.e.ii. General Options

The time series of biases evaluated at standard radiances can be regressed against the time (date) as the independent variable. The linear regression can be weighted by the calculated uncertainty on each bias. The regression coefficients including uncertainties (and their covariances) are calculated by the least squares method described in 5.b.ii. In this case, the variables, x_i and y_i are time series of Julian dates and radiance biases estimated in 5.c for each orbit since the most recent *trend reset*, respectively.

5.e.iii. Infrared GEO-LEO inter-satellite/inter-sensor Class

As above.

5.e.iv. Specifics for Prototype SEVIRI-IASI

Implemented as above.

5.f.   Generate Plots for GSICS Bias Monitoring

5.f.i.   Purpose

The results should be reported quantifying the magnitude of relative biases by inter-calibration. This should allow users to monitor changes in instrument calibration.

5.f.ii. General Options

Plots and tables of relative biases and uncertainties for standard radiances should be produced. These may show the evolution of the biases and their dependence on geophysical variables. These all results should be uploaded to the GSICS Data and Products server, and made available from the GPRC's appropriate inter-calibration webpage.

5.f.iii. Infrared GEO-LEO inter-satellite/inter-sensor Class

Plots should be regularly updated showing the relative brightness temperature biases for the standard radiances in each channel as time series with uncertainties. The trend line and monthly mean biases (and their uncertainties) should be calculated from these time series, following the example in Figure 12. This allows the most recent result to be tested for consistency with the series of previous results. If significant differences are found operators should be alerted, giving them the opportunity to investigate further.
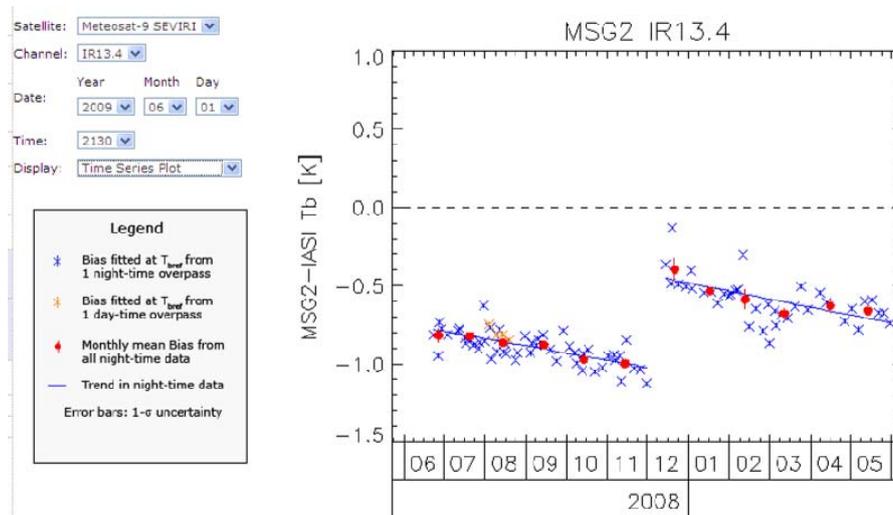

Figure 12: Example of time series plot showing relative bias of IR13.4 channel of Meteosat-9 and IASI at reference radiance following inset legend.

5.f.iv. Specifics for Prototype SEVIRI-IASI

This is implemented in the routine **icesi_plot_bias_ts** (see Annex A). The trends and statistics should be reset manually when decontamination procedures performed on MSG.
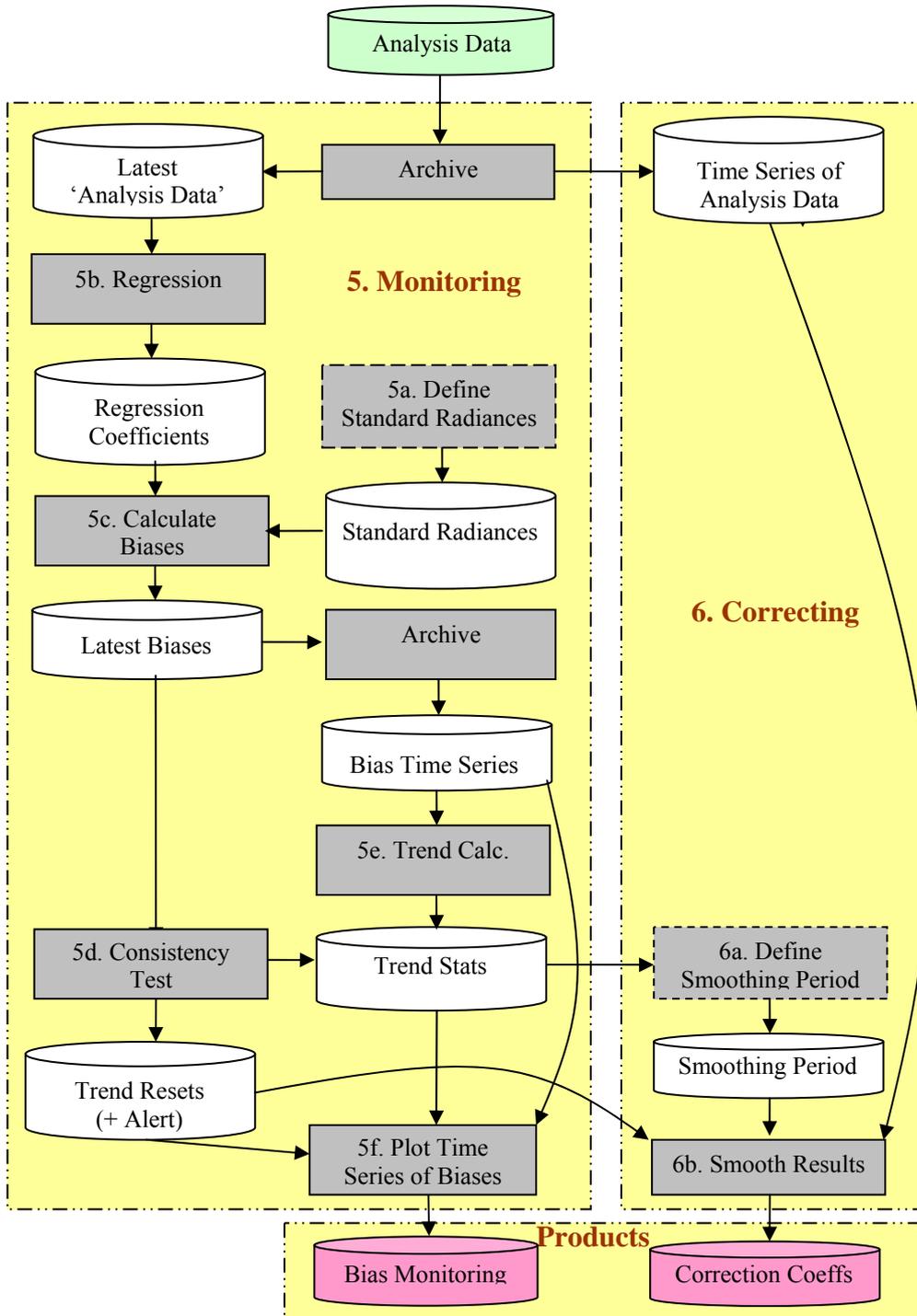
FLOW SUMMARY OF STEPS 5 AND 6 FOR SEVIRI-IASI

Figure 13: Summary of Recommended Data Flow within Steps 5 and 6 for SEVIRI-IASI

6. GSICS CORRECTION

This final step of the algorithm is to calculate the GSICS Correction, allowing the calibration of one instrument's observed data to be modified to become consistent with that of the reference instrument. The form of the GSICS Correction will be defined offline and can be instrument specific. However, application of the correction relies on the *Correction Coefficients* supplied by the inter-comparisons performed in the previous steps of the algorithm from the *Analysis Data*.
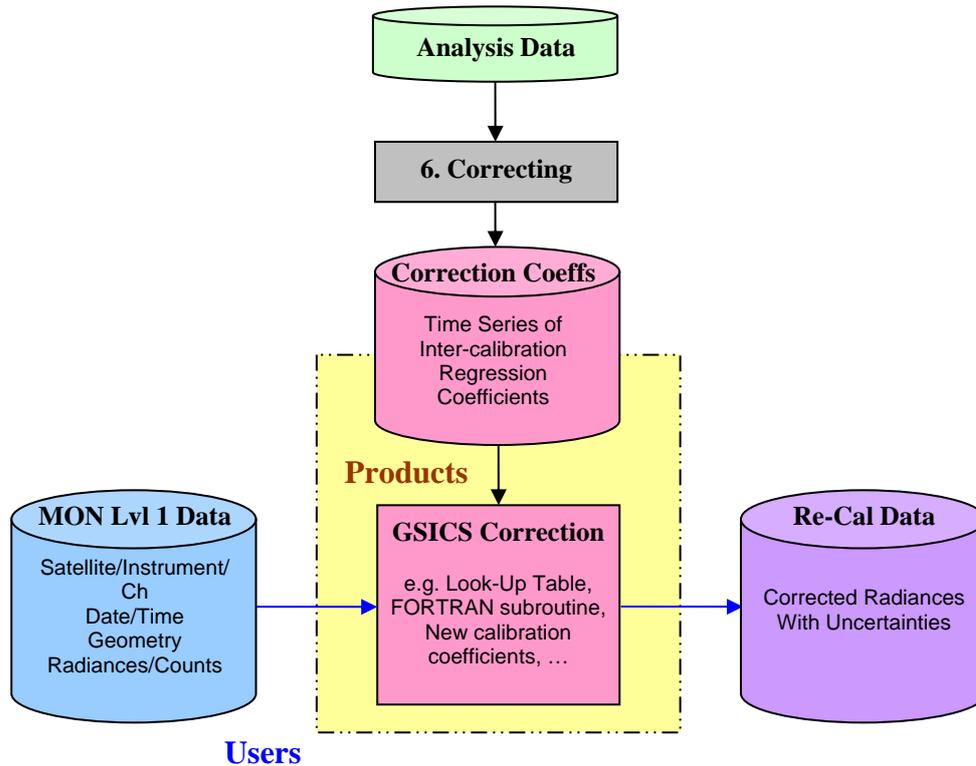

***Figure 14: Step 6 of Generic Data Flow, showing inputs and outputs,
and illustrating schematically how the correction could be applied by users.***

6.a. Define Smoothing Period (Offline)

6.a.i. Purpose

It is possible to combine data from a time series of inter-comparison results to reduce the random component of the uncertainty on the final GSICS Correction. (See 6.a). However, this requires us to define representative periods over which the results can be smoothed without introducing bias due to calibration drifts during the smoothing period. This period can be defined by comparing the observed rate of change of inter-comparison results with a pre-determined threshold, based on the required or achievable accuracy. In general, this definition is performed offline as it requires an in-depth analysis of the instruments' relative biases and consideration of likely explanatory mechanisms. However, it could also be fine-tuned in near real-time. The following describes the general approaches that should be implemented.

6.a.ii. General Options

In 5.e.ii, time series of radiance biases are regressed against date as the independent variable. This yields an estimate of the rate of change of bias with time, $\frac{d\Delta\hat{y}_{REF}}{dt}$, which can be compared to the threshold Δy_{max} to determine the smoothing period, τ_s:

Equation 15: $\tau_s = \Delta y_{\max}\left(\frac{d\Delta\hat{y}_{REF}}{dt}\right)^{-1}$

6.a.iii. Infrared GEO-LEO inter-satellite/inter-sensor Class

As above.

6.a.iv. Specifics for Prototype SEVIRI-IASI

Implemented as above.

The threshold value is taken to correspond to the typical uncertainty on the inter-comparison, which is equivalent to $\Delta y_{max}\equiv0.05$ K.

The SEVIRI channel with the highest rate of change is IR13.4, where $\frac{d\Delta\hat{y}_{REF}}{dt} \approx -0.1 K/month$.

This yields the following smoothing periods:

$\tau_s\approx14.5$ days for the Near Real-Time Correction
$\tau_s\approx29$ days for the Near Real-Time Correction (to match the orbital repeat cycle of Metop)

6.b.   Calculate Coefficients for GSICS Near-Real-Time Correction

6.b.i. Purpose

In order to reduce the random component of the uncertainty on the GSICS Correction, it is necessary to combine data from a time series of inter-comparison. The regression process described in 5.b is repeated using all the collocated radiances obtained over the smoothing period defined in 6.a. The resulting regression coefficients (and uncertainties) provide the *Correction Coefficients* used as input to the GSICS Correction. These regression coefficients are then used to evaluate the *Standard Bias* (also with uncertainties) at a set of *Standard Radiances*. The correction coefficients and standard biases are supplied in a netCDF format [defined at https://cs.star.nesdis.noaa.gov/GSICS/NetcdfConvention].

6.b.ii. General Options

All the collocation data within the smoothing period before and including the current date is combined and the regression of 5.b repeated on the aggregate dataset. This approach ensures all data is used optimally, with appropriate weighting according to its estimated uncertainty. This is the recommended approach in general for GSICS.

6.b.iii. Infrared GEO-LEO inter-satellite/inter-sensor Class

As above.

6.b.iv. Specifics for Prototype SEVIRI-IASI

Implemented as above, using a smoothing period t-14d to t-0 (where t is the current date) but using the following re-defined set of standard radiances for the IR channels SEVIRI on both Meteosat-8 and -9:

Ch (µm)	3.9	6.2	7.3	8.7	9.7	10.8	12.0	13.4
$T_{b\text{std}}$ (K)	284	236	255	284	261	286	285	267

6.c.   Calculate Coefficients for GSICS Re-Analysis Correction

6.c.i.   Purpose

In order to reduce the random component of the uncertainty on the GSICS Correction, it is necessary to combine data from a time series of inter-comparison. The regression process described in 5.b is repeated using all the collocated radiances obtained over the smoothing period defined in 6.a. The resulting regression coefficients (and uncertainties) provide the *Correction Coefficients* used as input to the GSICS Correction. These regression coefficients are then used to evaluate the *Standard Bias* (also with uncertainties) at a set of *Standard Radiances*. The correction coefficients and standard biases are supplied in a netCDF format [defined at https://cs.star.nesdis.noaa.gov/GSICS/NetcdfConvention].

However, because the smoothing period for the Re-Analysis Correction is defined to be symmetric about the validity date of the GSICS Correction coefficients, it is necessary to perform this step after a correspond delay of at least half the smoothing period after the validity date.

6.c.ii.   General Options

All the collocation data within the smoothing period before and including the current date is combined and the regression of 5.b repeated on the aggregate dataset. This approach ensures all data is used optimally, with appropriate weighting according to its estimated uncertainty. This is the recommended approach in general for GSICS.

6.c.iii. Infrared GEO-LEO inter-satellite/inter-sensor Class

As above.

6.c.iv. Specifics for Prototype SEVIRI-IASI

Implemented as above, using a smoothing period t-14d to t+14 (where t is the validity date) but using the following re-defined set of standard radiances for the IR channels SEVIRI on both Meteosat-8 and -9:

Ch (μm)	3.9	6.2	7.3	8.7	9.7	10.8	12.0	13.4
$T_{b\text{std}}$ (K)	284	236	255	284	261	286	285	267

References

Clough, S. A., and M. J. Iacono, 1995: Line-by-line calculations of atmospheric fluxes and cooling rates II: Application to carbon dioxide, ozone, methane, nitrous oxide, and the halocarbons. J. Geophys. Res., 100. 16519-16535.

EUMETSAT, 2006: MSG SEVIRI Spectral Response Characterisation, EUM/MSG/TEN/06/0010.

EUMETSAT, 2007, Typical Radiometric Accuracy and Noise for MSG-1/2, EUM/OPS/TEN/07/0314, http://www.eumetsat.int/idcplg?IdcService=GET_FILE&dDocName=pdf_typ_radiomet_acc_msg-1-2&RevisionSelectionMethod=LatestReleased

EUMETSAT, 2008a: IASI Level 1 Products Guide, Ref.: EUM/OPS-EPS/MAN/04/0032, http://oiswww.eumetsat.org/WEBOPS/eps-pg/IASI-L1/IASIL1-PG-4ProdOverview.htm#TOC411

EUMETSAT, 2009: ATBD for EUMETSAT's Inter-Calibration of SEVIRI-IASI, EUM/MET/REP/08/0468.

EUMETSAT, 2010: GSICS SEVIRI-IASI Inter-calibration Uncertainty Analysis, EUM/MET/TEN/09/0668.

EUMETSAT, 2008b: Effective Radiance and Brightness Temperature Relation for Meteosat 8 and 9, EUM/OPS-MSG/TEN/08/0024.

Hewison, T.J., 2009a: Quantifying the Impact of Scene Variability on Inter-Calibration, GSICS Quarterly, Vol. 3, No. 2, 2009.

Hewison, T. J., 2008a: SEVIRI/IASI Differences in 2007, GSICS Quarterly, Vol.2, No.1, 2008. (Available online).

Hewison, T.J., 2008b: The Inter-calibration of Meteosat and IASI during 2007, EUMETSAT Internal Report, April 2008 (Available online).

Hewison, T.J. and M. König, 2008: Inter-Calibration of Meteosat Imagers and IASI, Proceedings of EUMETSAT Satellite Conference, Darmstadt, Germany, September 2008. (Available online).

König, M., 2007: Inter-Calibration of IASI with MSG-1/2 onboard METEOSAT-8/9, GSICS Quarterly, Vol.1, No.2, August 2007 (Available online).

Minnis, P., A. V. Gambheer, and D. R. Doelling, 2004: Azimuthal anisotropy of longwave and infrared window radiances from CERES TRMM and Terra data. *J. Geophys. Res.*, **109**, D08202, doi:10.1029/2003JD004471.

Press, W.H., S.Teukolksy, W.T.Vetterling and B.Flannery, 1995: Numerical recipes: the art of scientific computing, Second edition, Cambridge University Press.

Rothman et al., 2003: The HITRAN molecular spectroscopic database: edition of 2000 including updates through 2001, Journal of Quantitative Spectroscopy and Radiative Transfer. vol. 82, 5-44.

Tahara, Yoshihiko, 2008: New Approach to Intercalibration Using High Spectral Resolution Sounder, Meteorological Satellite Center Technical Note, No. 50, 1-14.

Tahara, Yoshihiko and Koji Kato, 2009: New Spectral Compensation Method for Intercalibration Using High Spectral Resolution Sounder, Meteorological Satellite Center Technical Note, No. 52, 1-37.

Tobin, D. C., H. E. Revercomb, C. C. Moeller, and T. Pagano, 2006: Use of Atmospheric Infrared Sounder high-spectral resolution spectra to assess the calibration of Moderate re solution Imaging Spectroradiometer on EOS Aqua, *J. Geophys. Res*., **111**, D09S05, doi:10.1029/2005JD006095.

Wu, X., 2009: GSICS GOES-AIRS Inter-Calibration Algorithm at NOAA GPRC, Draft version dated January 5, 2009.

ANNEX A - INTER-CALIBRATION (EUMETSAT) OF SEVIRI-IASI (ICESI) V0.3
These routines and netCDF data formats will be documented in detail in a separate document. This is an extract for information.

A.1. Overview of Data Flow
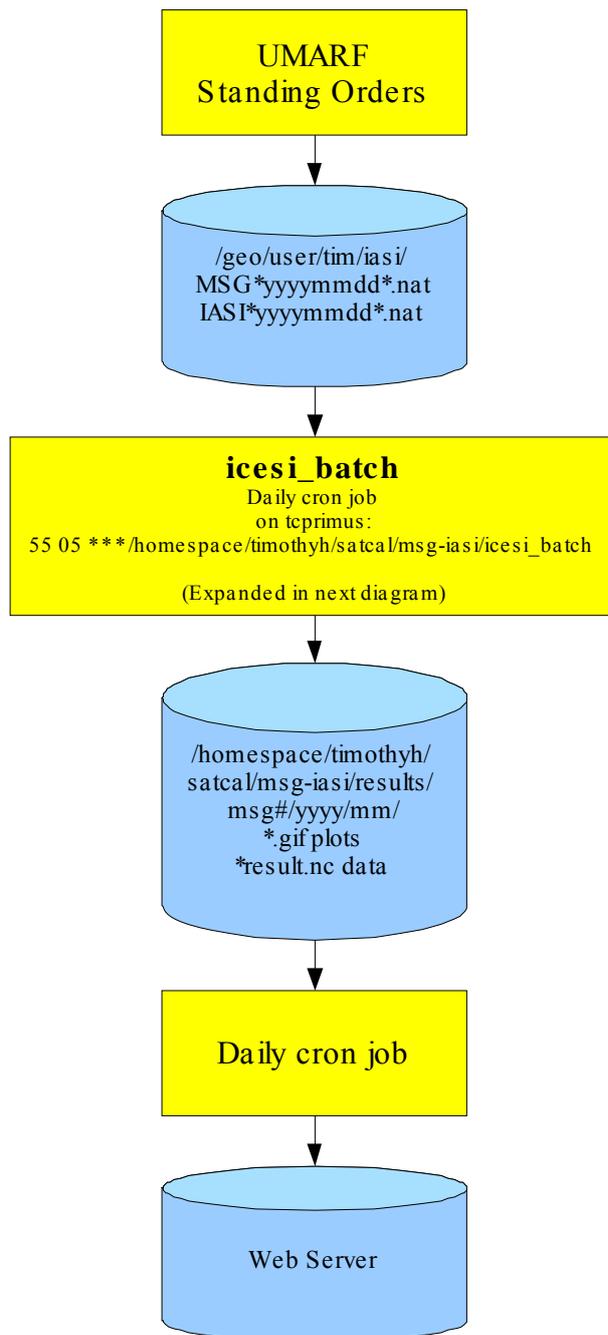
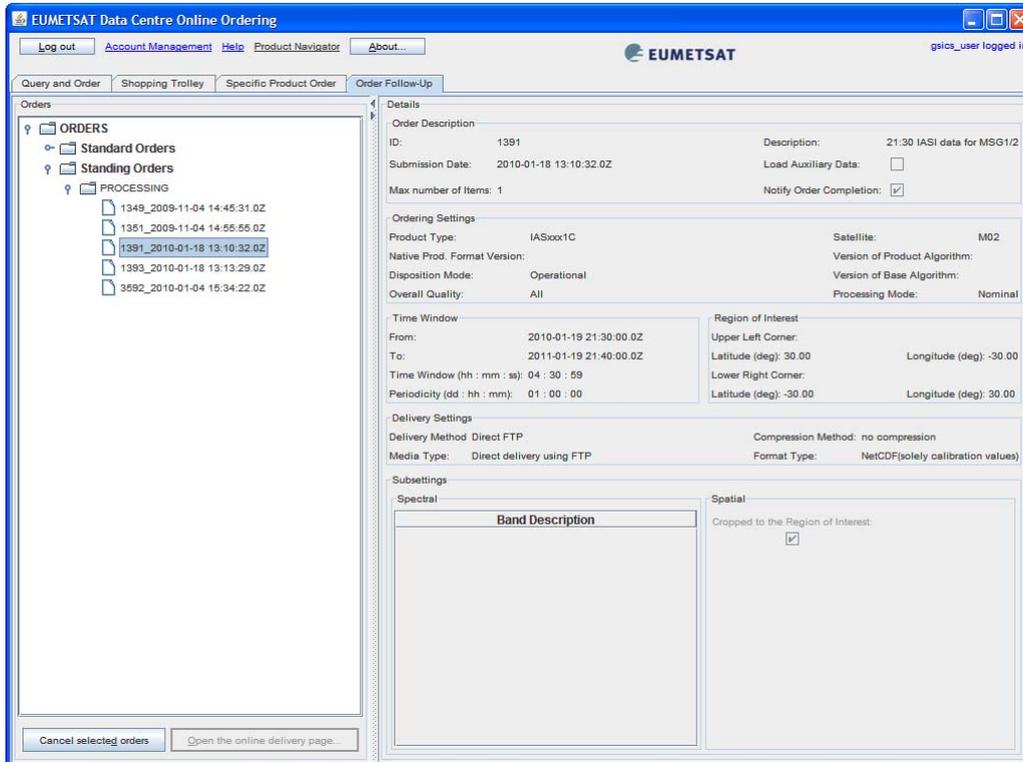## A.2. Input Satellite Data – EUMETSAT Data Centre Standing Order

Figure 15 – Standing Order to supply IASI data to GSICS Data and Products Server
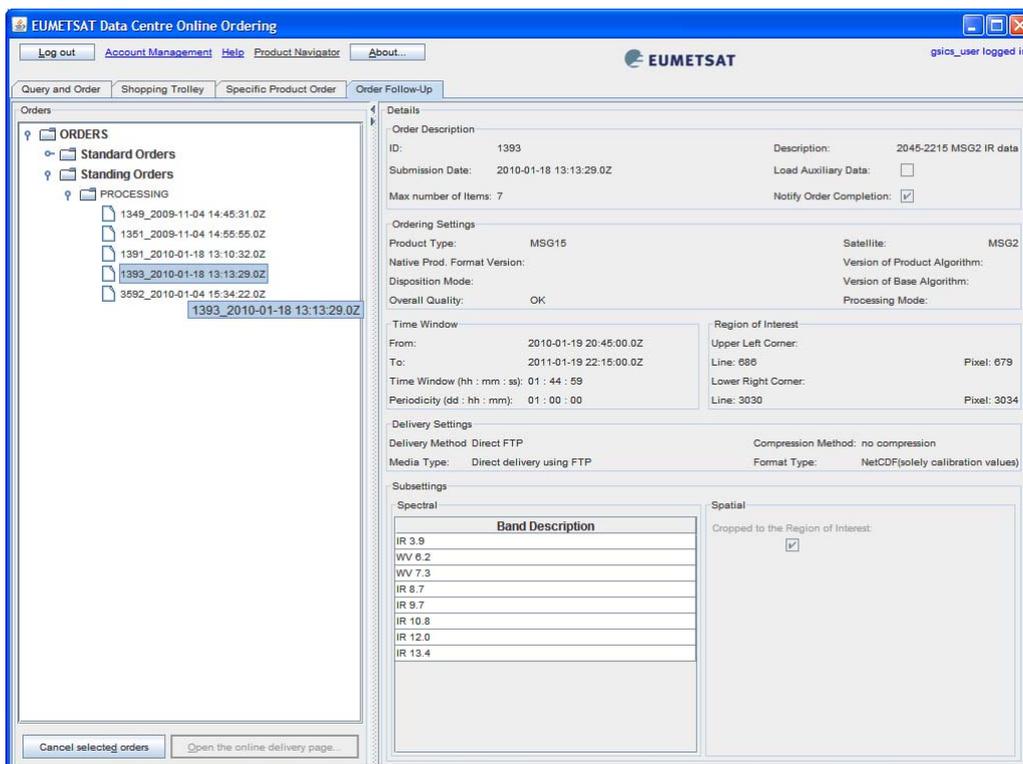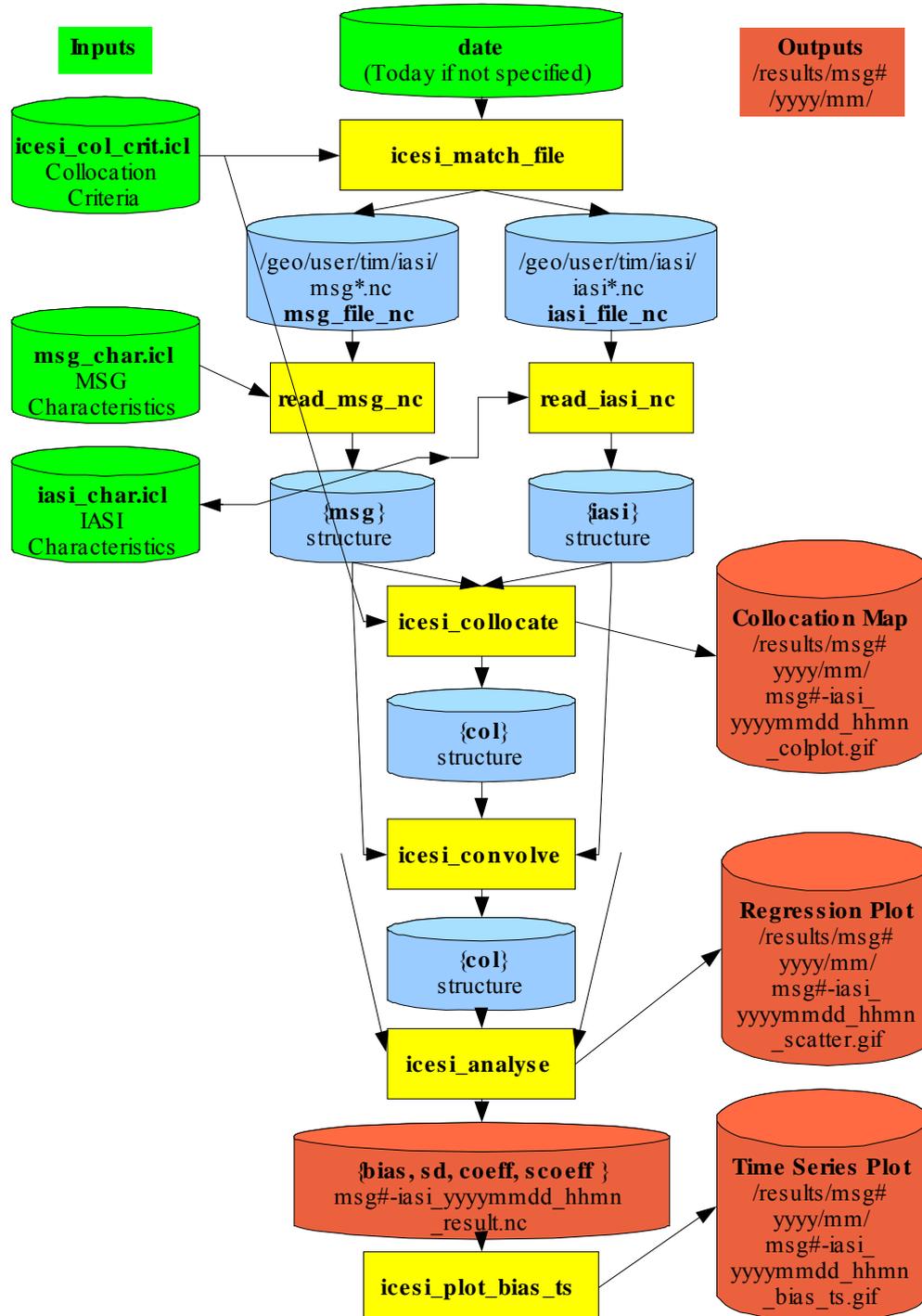

Figure 16 – Standing Order to supply MSG2 data to GSICS Data and Products Server

A.3. Detail of Inter-Calibration Processing ICESI_BATCH

A.4. Configuration Options

The data saved for each collocation should be comprehensive to facilitate future down selection, analysis, and certain reprocessing (e.g., spectral convolution). It should contain all the GEO and LEO data, as well as the metadata regarding the collocation.